GEOPHYSICS

Upper and lower plate controls on the great 2011 Tohoku-oki earthquake

Xin Liu[1,2]* and Dapeng Zhao[1]*

Copyright © 2018 The Authors, some rights reserved; exclusive licensee American Association for the Advancement of Science. No claim to original U.S. Government Works. Distributed under a Creative Commons Attribution NonCommercial License 4.0 (CC BY-NC).

The great 2011 Tohoku-oki earthquake [moment magnitude (M_w) 9.0)] is the best-documented megathrust earthquake in the world, but its causal mechanism is still in controversy because of the poor state of knowledge on the nature of the megathrust zone. We constrain the structure of the Tohoku forearc using seismic tomography, residual topography, and gravity data, which reveal a close relationship between structural heterogeneities in and around the megathrust zone and rupture processes of the 2011 Tohoku-oki earthquake. Its mainshock nucleated in an area with high seismic velocity, low seismic attenuation, and strong seismic coupling, probably indicating a large asperity (or a cluster of asperities) in the megathrust zone. Strong coseismic high-frequency radiations also occurred in high-velocity patches, whereas large afterslips took plate in low-velocity areas, differences that may reflect changes in fault friction and lithological variations. These structural heterogeneities in and around the Tohoku megathrust originate from both the overriding and subducting plates, which controlled the nucleation and rupture processes of the 2011 Tohoku-oki earthquake.

INTRODUCTION

The great Tohoku-oki earthquake [moment magnitude (M_w 9.0)] on 11 March 2011 occurred in a megathrust zone formed by the active subduction of the Pacific plate beneath the Okhotsk plate along the Japan Trench (Fig. 1). The seaward updip limit of the Tohoku megathrust reaches the Japan Trench, according to the occurrence of large near-trench slips during the 2011 Tohoku-oki earthquake with a devastating tsunami (*1*). All the large megathrust earthquakes ($M_w \geq$ 7.0) during the past 100 years beneath the Tohoku forearc nucleated in a depth range of ~10 to 40 km (Fig. 1). The landward downdip limit of the megathrust zone is located at ~50-km depth, as estimated from the interplate seismicity (*2*).

Although the 2011 Tohoku-oki earthquake is the best instrumentally recorded megathrust earthquake ($M_w \geq$ 9.0) in the world, its causal mechanism is still a matter of controversy. Early tomographic studies (*3*, *4*) of the Tohoku subduction zone showed that the 2011 Tohoku-oki mainshock hypocenter was located in a significant high-velocity (high-V) area, suggesting the possibility of a mechanically strong patch in the megathrust zone, where tectonic stress accumulated for a long time because of the strong coupling between the subducting Pacific slab and the overriding Okhotsk plate (*5*, *6*). Subsequent tomographic studies (*7*–*9*) confirmed such a structural feature and suggested that the anomaly may reflect topographic and/or compositional variations on the subducting Pacific slab. However, some authors have argued that the subduction of rough seafloor relief would cause fault creep and have proposed that the 2011 Tohoku-oki earthquake occurred in an area of relatively smooth subducting seafloor (*10*). Analysis of heat flow data (*11*) shows a relatively lower apparent coefficient of friction, suggesting a weaker megathrust zone producing the 2011 Tohoku-oki earthquake. Bletery *et al.* (*12*) also suggested that the Tohoku megathrust has a relatively homogeneous shear strength. Recently, using residual topography and gravity data, Bassett *et al.* (*13*) proposed that variations in the forearc lithology of the overriding plate were the main cause of along-strike variations in the Tohoku-oki slip behavior. Spatial variations of stress orientation on the Tohoku megathrust show a correlation with spatial variations in coupling, with locked areas stronger than creeping areas in the megathrust zone (*14*). We suggest that this ongoing controversy is mainly due to the poor state of knowledge of the megathrust zone beneath the Tohoku forearc.

More than two decades ago, sP depth phases (fig. S1) were detected from seismograms of suboceanic earthquakes in the Tohoku forearc recorded by the permanent seismic network installed on Honshu Island (*15*). Because the sP depth phases are very useful for locating earthquakes that occur outside a seismic network (fig. S1), this discovery of sP depth phases at short epicentral distances laid the foundation for precisely locating suboceanic earthquakes and mapping the three-dimensional (3D) seismic structure of the entire Tohoku forearc beneath the Pacific Ocean where only a few ocean bottom seismometers (OBSs) are deployed. Some researchers (*16*, *17*) have used data recorded at some portable OBS stations to investigate seismic structures of a few small areas in the Tohoku forearc.

Using arrival-time data of the suboceanic earthquakes relocated with the sP depth phases, Zhao *et al.* (*18*) determined the first 3D P-wave velocity (V_p) model of the entire Tohoku forearc from the Japan Trench to the Pacific coast. Since then, structural heterogeneities in the Tohoku forearc have been revealed and imaged in more and more detail by applying this approach to a much larger body of data of precisely relocated suboceanic events (*3*, *4*, *7*–*9*). The most important and exclusive contribution of these tomographic studies is the detection of along-trench structural variations in and around the Tohoku megathrust, in addition to the along-dip variations (*19*), though there is doubt about the vertical resolution of these tomographic images (*10*).

Recently, an abrupt southwest-northeast (SW-NE)–striking boundary was identified in the Tohoku forearc (the magenta lines in Figs. 2 and 3), across which the residual topography and gravity anomalies increase from the south to the north (*13*). This forearc segment boundary (FSB) was associated with the offshore continuation of the Median Tectonic Line, with gravity, bathymetry, and density anomalies associated with the lithologic juxtaposition of accretionary complexes (south) and granitic batholiths (north) expressed in onshore geology (*13*). However, the depth resolution of the residual gravity data is much lower than that of seismic tomography. The residual topography and gravity anomalies may be only sensitive to the forearc crustal structure, and so only density

[1]Department of Geophysics, Tohoku University, Sendai 980-8578, Japan. [2]Key Lab of Submarine Geosciences and Prospecting Techniques, Ministry of Education, and College of Marine Geosciences, Ocean University of China, Qingdao 266100, China. *Corresponding author. Email: liuxin@ouc.edu.cn (X.L.); zhao@tohoku.ac.jp (D.Z.)

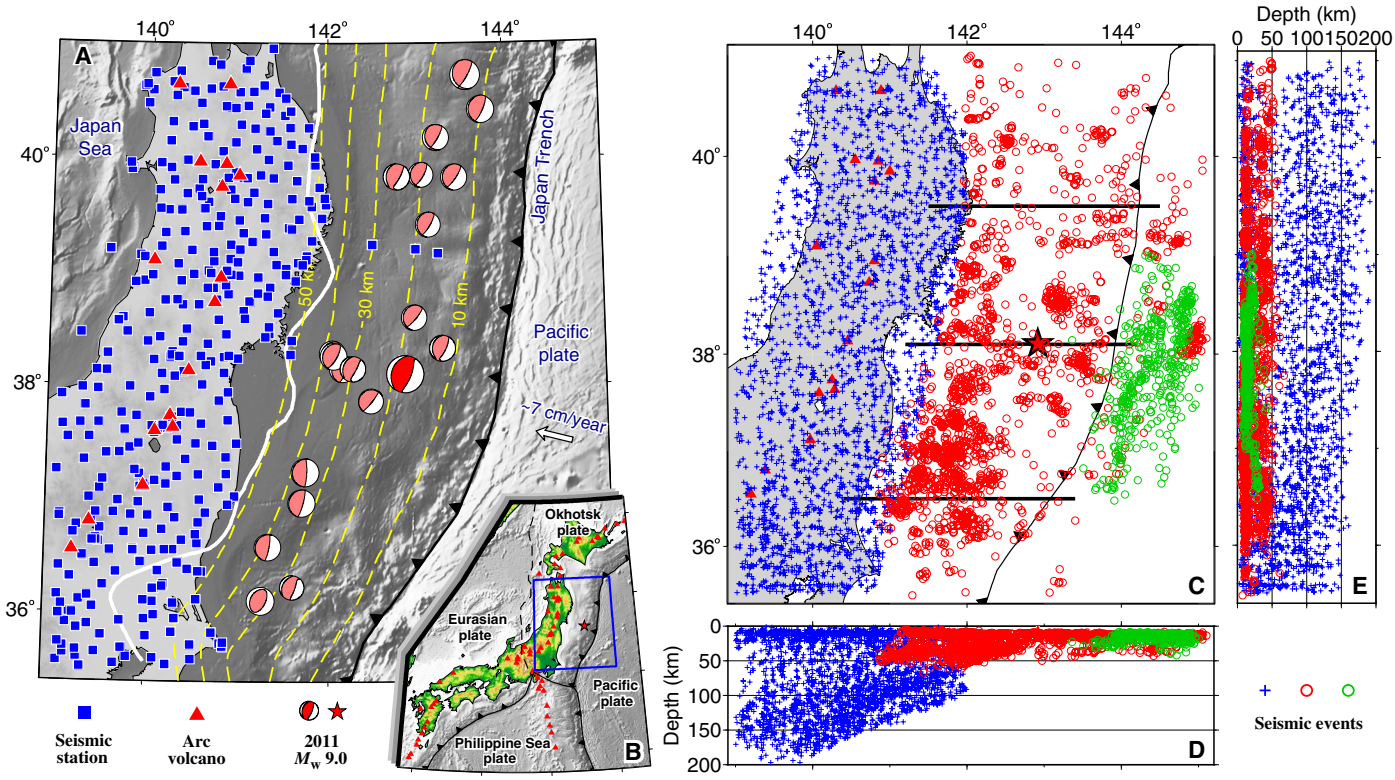

Fig. 1. Seismic stations and earthquakes used in this study. (**A**) Distribution of the 382 seismic stations (blue squares) used in this study. The red beach ball denotes the focal mechanism of the great 2011 Tohoku-oki earthquake (M_w 9.0), whereas the pink beach balls denote focal mechanisms of other megathrust earthquakes ($M_w \geq$ 7.0) during 1917 to 2017. The white line marks the downdip limit of interplate seismicity (*2*). The yellow dashed lines denote depth contours of the UBP. (**B**) Tectonic settings of the study region (blue box). (**C**) Map view showing the distribution of 4760 local earthquakes used in this study. The blue crosses denote 2537 events that occurred beneath the seismic network (*9*). The red circles show 1788 events that occurred under the Pacific Ocean and were relocated using sP depth phase data (*7*, *48*). The green circles denote 435 suboceanic events located using OBS data (*49*). The three black lines denote locations of the vertical cross sections in Fig. 5. (**D**) East-west and (**E**) north-south vertical cross sections of the 4760 earthquakes shown in (C). The red triangles in (A) to (C) denote active arc volcanoes. The red star in (B) and (C) denotes the mainshock epicenter of the 2011 Tohoku-oki earthquake (M_w 9.0).

anomalies in the forearc crust, not the mantle wedge, were calculated using the residual gravity anomalies (*13*). The intersection of the forearc Moho in the overriding Okhotsk plate with the subducting Pacific plate is located at ~20- to 30-km depths, much shallower than the downdip limit of the Tohoku megathrust at ~50-km depth (*2*). Therefore, the residual topography and gravity anomalies obtained (*13*) cannot constrain the structure of the deeper portion of the Tohoku megathrust (at depths of ~30 to 50 km).

To better understand the causal mechanism of the 2011 Tohoku-oki earthquake, here we revisit the Tohoku forearc structure using high-resolution seismic tomography. Our new tomographic model shows a high correlation with the residual topography and gravity data in the Tohoku forearc (*13*). We find a close link between structural heterogeneities in and around the megathrust zone and the rupture process of the 2011 Tohoku-oki earthquake, a discovery that sheds new light on the causal mechanism of megathrust earthquakes.

RESULTS

Our new tomographic images (Figs. 2 to 5) show significant along-trench V_p variations that are similar to those of the previous tomographic models (*3*, *4*, *7*–*9*), whereas our new model has a much better depth resolution (~5 to 10 km) as confirmed by the detailed resolution tests (figs. S2 to S7). We were able to make these advances by adopting a novel strategy for the 3D grid setting to achieve the best vertical resolution with our data set (see Materials and Methods for details).

Here, we reanalyze the residual topography and gravity data in the Tohoku forearc (*13*) and compare them with the new V_p tomography obtained by this study (Figs. 2 and 3). The V_p image along the upper boundary of the subducting Pacific plate (UBP) from the new 3D V_p model mainly reflects V_p variations along the Tohoku megathrust (Fig. 2C). A 2D V_p model above the UBP is derived from the 3D V_p model (see Materials and Methods for details), which generally represents the average V_p variations in the overriding Okhotsk plate (Fig. 2D).

From the Japan Trench axis to the 10-km depth contour of the UBP, the patterns of the residual topography and gravity anomalies are different from that of the V_p image, especially in the area north of ~39°N (Fig. 2 and fig. S8). In the shallow portion (less than ~10-km depth) of the megathrust zone, active-source seismic profiles have a much higher resolution (*20*, *21*), which revealed a strong along-trench variation of the subducting sediment thickness, in particular, the subducting sediments around ~38°N appear to be much thinner than those in the other areas (fig. S9). This feature should be partly responsible for (or affect) the along-trench velocity variation revealed by our V_p tomography (Fig. 2C) and previous tomographic results (*3*, *7*), that is, the velocity appears slightly higher around ~38°N than the other

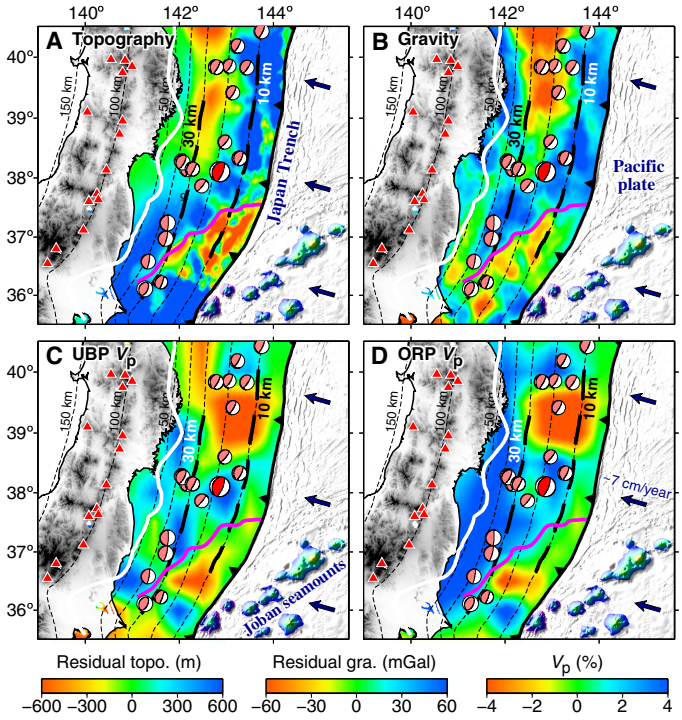

Fig. 2. Forearc anomalies in the Tohoku subduction zone. (**A**) Residual topography and (**B**) residual gravity derived from Bassett *et al.* (*13*). (**C**) P-wave velocity (V_p) tomography along the UBP and (**D**) average 2D V_p image of the overriding plate (ORP) obtained by this study. The magenta line marks the FSB proposed by Bassett *et al.* (*13*). The other labeling is the same as that in Fig. 1.

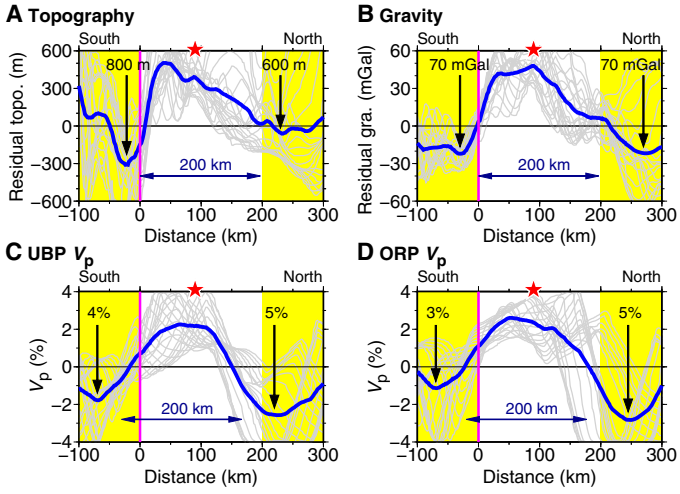

Fig. 3. Anomalies in the source area of the 2011 Tohoku-oki earthquake. (**A**) Residual topography and (**B**) residual gravity in the Tohoku forearc (*13*). (**C**) P-wave velocity (V_p) variations along the UBP and (**D**) average V_p variations of the ORP obtained by this study. Gray lines in (A) to (D) show profiles along the UBP depth contours of 10 to 30 km (black bold dashed lines in Fig. 2) with an interval of 1 km. The horizontal axes show the distance of points along the profiles from the FSB (the magenta line). The blue line denotes the mean of each ensemble of profiles (gray lines). The red star denotes the epicenter location of the great 2011 Tohoku-oki earthquake (M_w 9.0).

parts of the shallow portion of the megathrust zone (Fig. 2C), though the tomographic resolution is lower than that of the active-source seismic surveys. Although the thickness of the sedimentary layer is smaller than the tomographic resolution scale (~5 to 10 km), the V_p of the sediment (~1.5 to 4.0 km/s) is much lower than that of the rocks above and below the sedimentary layer (fig. S9). Thus, a P wave would take considerable travel time when it passes through the sedimentary layer. Hence, the effect of the sedimentary layer on the tomographic image is not trivial.

We prefer to use the results (fig. S9) of active-source seismic surveys (*20*, *21*) and our tomographic model (Fig. 2C) to constrain the shallow structure of the megathrust zone. Although the patterns of the residual topography and gravity anomalies are different from that of the seismic images in the shallow portion of the Tohoku megathrust, distinct along-trench variations in the residual topography and gravity are visible across the FSB (*13*) near the Japan Trench (Fig. 2).

Between the 10- and 30-km depth contours of the UBP, the following features are visible (Figs. 2 and 3 and fig. S8). (i) The patterns of the residual topography and gravity anomalies are similar to those of the V_p images. (ii) A SW-NE–striking high-topography, high-gravity, and high-V zone exists around ~37°N to 38°N, with a length of ~100 to 200 km along the trench. (iii) The residual topography, gravity, and V_p anomalies increase from the south to the north across the FSB, and after reaching their maximum, they all decrease toward the north with a similar amplitude but shallower gradient as their increases. (iv) The residual topography and gravity anomalies (Fig. 2, A and B) are more similar (with higher correlation coefficients as shown in fig. S8) to the V_p image along the UBP (Fig. 2C) than the average V_p image of the overriding plate (Fig. 2D). These features suggest that the residual topography and gravity anomalies between the 10- and 30-km UBP depth contours reflect not only lithological variations of the overriding plate (*13*) but also V_p variations of the megathrust at 10- to 30-km depths. These similar patterns of the different anomalies in the Tohoku forearc indicate the existence of significant along-trench structural heterogeneity in and around the Tohoku megathrust at ~10- to 30-km depths.

Between the 30- and 50-km depth contours of the UBP, the patterns of the residual topography, gravity, and V_p anomalies are generally different from each other (Fig. 2 and fig. S8); hence, we prefer to use the 3D V_p model to constrain the deeper structure of the Tohoku megathrust (at 30- to 50-km depths). In this portion, our tomographic image (Fig. 2C) shows high-V anomalies from ~36°N to ~39°N, whereas low-velocity (low-V) anomalies exist south of ~36°N and north of ~39°N. Such a feature indicates along-trench structural heterogeneities, such as variations in lithology and/or pore fluid contents, in the deeper portion of the Tohoku megathrust.

In summary, active-source seismic surveys (*20*, *21*), residual topography and gravity anomalies (*13*), and our tomographic results all reveal distinct along-trench structural variations in and around the Tohoku megathrust from the Japan Trench down to a depth of ~50 km under the Pacific coast (Figs. 2 and 3). These along-trench structural variations may be related to the heterogeneous interplate coupling revealed by geodetic measurements (Fig. 4A) (*5*, *6*). The spatial variations in coupling at the Tohoku megathrust are also correlated with spatial variations of stress orientation, with creeping parts having a lower friction coefficient than locked parts (*14*). Modeling of surface heat flow data suggested a weaker Tohoku megathrust (*11*), but most of the heat-flow data from the Japan Trench to the Pacific coast are located above the low-V and weak coupling patches (creeping parts) in the Tohoku megathrust (Fig. 4A). Only one heat-flow site (*11*) is located above the high-V and strong coupling patch (locked parts) around ~38°N

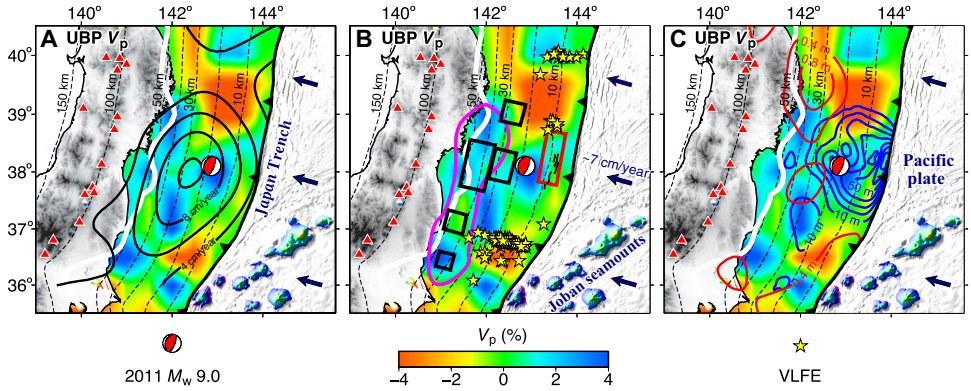

Fig. 4. V_p tomography and characteristics of the 2011 Tohoku-oki earthquake. The colors in (**A** to **C**) show V_p tomography along the UBP obtained by this study. Black bold contour lines in (A) denote the back-slip rate (*5*). In (B), the yellow stars mark epicenters of very low frequency earthquakes (VLFEs) (*24*); the red rectangle denotes a slow slip event (*22*) preceding the 2011 Tohoku-oki earthquake; the black rectangles show locations of coseismic strong ground motions (*39*); the magenta contour line marks the site of coseismic high-frequency P-wave radiation with a relatively low seismic moment during the 2011 Tohoku-oki earthquake (*40*); and the black short lines near the trench indicate seafloor traces of normal faults (*34*). The blue and red contour lines in (C) denote the coseismic slip (*1*) and the afterslip (*43*), respectively. The other labeling is the same as that in Fig. 2.

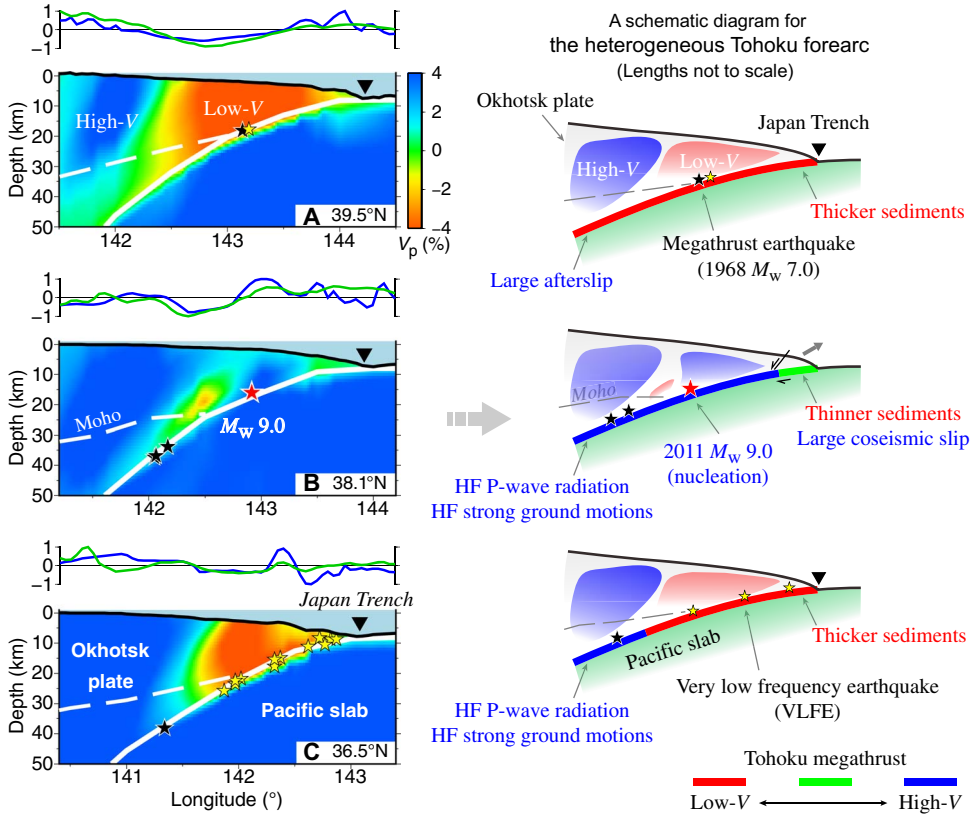

Fig. 5. Vertical cross sections of V_p tomography (left) and corresponding cartoons (right). The east-west vertical cross sections are along the three profiles shown in Fig. 1C. The normalized residual topography (blue line) and gravity (green line) along each profile are shown atop each cross section. The red and blue colors in (**A** to **C**) denote low and high V_p perturbations, respectively, whose scale is shown beside (A). The white bold and dashed lines in (A) to (C) denote the UBP and the forearc Moho, respectively. The red star denotes the mainshock hypocenter of the 2011 Tohoku-oki earthquake (M_w 9.0). The black and yellow stars indicate other megathrust earthquakes (M_w 7.0 to 8.0) during 1917 to 2017 and the VLFEs (*24*) within a 40-km width of each profile, respectively. Note that the hypocenters of the VLFEs and the megathrust earthquakes are set on the UBP, because their accurate focal depths are unclear for most of them. The reverse triangle denotes the Japan Trench axis. HF, high-frequency. In the right panels, the red, green, and blue lines denote low-, normal-, and high-V_p anomalies atop the subducting Pacific plate, respectively, according to the tomographic results of this study. The gray dashed line denotes the forearc Moho.

in the megathrust zone (Fig. 4A). Thus, the heat dissipation model (*11*) cannot fully describe the along-trench heterogeneities beneath the Tohoku forearc.

DISCUSSION

The preceding deformation, coseismic slip, high-frequency radiation, and postseismic deformation of the 2011 Tohoku-oki earthquake (M_w 9.0) have been well documented using various approaches and data sets. Previous studies have suggested that the structural heterogeneities in the megathrust zone may control the nucleation and coseismic slip of the 2011 Tohoku-oki earthquake (*4*, *7*, *9*). Our present results show that the 2011 Tohoku-oki earthquake (M_w 9.0) and other megathrust earthquakes ($M_w \geq 7.0$) in the past 100 years (1917–2017) are all located in or close to the high-*V* zones in the Tohoku megathrust (Fig. 2C). The high-*V* zone in the M_w 9.0 mainshock area also exhibits a high-*Q* (low attenuation) anomaly (*8*, *9*) and strong seismic coupling (Fig. 4A). This high-*V*, high-*Q*, and strong coupling patch may indicate a mechanically strong area in the Tohoku megathrust, which may be responsible for the nucleation of the 2011 Tohoku-oki earthquake (*4*), as well as the preceding seismicity and slow earthquakes around the source area (Fig. 4B) (*22*, *23*). This large asperity in the Tohoku megathrust may result from both the granitic batholiths in the overriding Okhotsk plate (*13*) and anomalies atop the subducting Pacific plate, such as variations in the sediment volume (Figs. 2C and 5B and fig. S9) (*4*, *7*). On the other hand, many very low frequency earthquakes (VLFEs) also took place in the Tohoku forearc (*24*). In contrast to the megathrust earthquakes, the VLFEs seem mainly located in or close to the low-*V* patches in the megathrust zone (Fig. 4B), which generally exhibit low-*Q* (high attenuation) anomalies (*8*, *9*) and weak seismic coupling (Fig. 4A). The low-*V*, low-*Q*, and weak coupling patches may indicate more pore fluids near the Tohoku megathrust, variations in lithology and the presence of accretionary complexes in the overriding plate (*13*), and/or thicker sediment volumes atop the subducting plate (*4*, *7*). These features indicate that structural heterogeneities in both the upper and lower plates control the nucleation of the megathrust earthquakes and even the VLFEs.

One of the most significant features of the 2011 Tohoku-oki earthquake is the large coseismic slip (LCS) near the Japan Trench (*1*), where a stable sliding zone should exist with only slow earthquakes including tsunami earthquakes (*19*). The Japan Trench Fast Drilling Project (JFAST) drilled into the Tohoku megathrust in the LCS area (*25*), which revealed a low friction and a low shear stress in the shallow portion of the megathrust zone (*26*, *27*). Hence, a shallow big asperity or a strong patch may not exist near the trench (*28*). The LCS near the trench may result from dynamic weakening processes such as the thermal pressurization of pore fluid (*29*), which may be promoted by low permeability of the shallow portion of the Tohoku megathrust (*30*). The JFAST core analyses show that an interval of smectite-rich, pelagic clay with velocity-strengthening and velocity-weakening frictional behavior exists in the shallow megathrust zone (*31*). Recent friction experiments using a core sample from the JFAST show that an increase in sliding velocity can induce a change from steady-state frictional strength or slip-strengthening friction to slip-weakening frictional behavior (*32*). However, Scholz (*33*) argued that explanations of involving thermal weakening mechanisms to overcome velocity strengthening cannot result in a total stress drop as revealed by a prominent landward-dipping normal fault that slipped during the 2011 Tohoku-oki earthquake (*34*), a series of strong normal-faulting aftershocks in the overriding plate and the megathrust zone (*35*), and almost no interplate thrust earthquakes in the LCS area after the mainshock until at least the end of 2013 (*36*). Scholz (*33*) proposed that the bimaterial effect with a more compliant overriding plate could overcome velocity strengthening by reducing the normal stress and lead to the rupture propagating as a wrinkle pulse. Around the LCS area, seismic surveys and the JFAST core samples have revealed a compliant (low-*V*) prism in the overriding plate (*37*), whereas our tomographic results show that normal- to high-*V* anomalies exist atop the subducting Pacific slab (Fig. 4C), which may reflect a thinner sediment layer around the LCS area (*7*), as revealed by the seismic surveys (fig. S9) (*20*, *21*). A thin sediment layer may increase the contrast of elastic constants between the compliant prism and the subducting plate, favoring a wrinkle pulse rupture mode (Fig. 5) (*33*). In addition, a torqueing mechanism for thrust fault rupture near the free surface (*38*) may further reduce the normal stress on the shallow portion of the Tohoku megathrust, leading to an LCS near the Japan Trench.

In contrast to the LCS with weak high-frequency radiation near the trench, the sites of strong high-frequency radiation and strong ground motions of the 2011 Tohoku-oki earthquake are mainly located in the deeper portion of the megathrust zone beneath the Pacific coast where relatively modest coseismic slips occurred (*39*, *40*). Such a depth-varying rupture process has been related to fault properties along-dip in the Tohoku megathrust (*19*). Depth-varying source spectra and path attenuation may account for the strong high-frequency radiation beneath the Pacific coast (*41*), where visible high-*Q* anomalies exist in and around the megathrust (*8*, *9*). Our tomographic results show that the sites of strong high-frequency radiation and strong ground motions in the deeper portion (~30- to 50-km depth) of the Tohoku megathrust from ~36°N to ~39°N mainly exhibit high-*V* anomalies, whereas visible low-*V* anomalies exist south of ~36°N and north of ~39°N in the megathrust zone in the same depth range (Figs. 4B and 5). These velocity variations may reflect along-trench changes in the fault property, such as variations in lithology and/or pore fluid contents, in the deeper portion of the Tohoku megathrust, which have a close relationship with or even control the distribution of high-frequency radiation of the 2011 Tohoku-oki earthquake, in addition to the along-dip variation of the fault property (*19*).

The along-trench varying postseismic deformation of the 2011 Tohoku-oki earthquake is mainly caused by viscoelastic relaxation and afterslip (*42*–*45*). The viscoelastic relaxation mainly depends on the viscosity structure of the subduction zone, which should have a close relationship with the seismic velocity and attenuation structures revealed by tomographic studies. Our results show an obvious high-*V* mantle wedge nose beneath the Tohoku forearc (Fig. 5), which also exhibits a high-*Q* anomaly (*8*). Such a feature probably indicates a cold and high-viscosity mantle wedge nose, which may play an important role in the viscoelastic relaxation (*44*). Although our local-earthquake tomography cannot reveal a thin weak (low-*V*) layer beneath the Pacific plate (*42*), or within the lower half of the plate (*44*), which may account for the landward seafloor postseismic displacements of the M_w 9.0 earthquake, a sheet-like low-*V* zone has been imaged under the Pacific slab beneath Tohoku by regional mantle tomography of East Asia (*46*). The afterslip of the 2011 Tohoku-oki earthquake mainly occurred in areas surrounding the coseismic rupture, which may result from the difference in frictional and material properties in the megathrust zone (*1*, *43*). Our results show that the large afterslip areas (≥0.8 m) generally exhibit low-*V* anomalies in the megathrust zone, in contrast to the visible high-*V* anomalies in the coseismic slip area (≥10 m) (Figs. 4C and 5). These features indicate that the along-trench structural heterogeneities in and around the Tohoku megathrust revealed by this study may also

account for the along-trench variations in postseismic deformation of the 2011 Tohoku-oki earthquake.

CONCLUSION

To clarify the causal mechanism of the 2011 Tohoku-oki earthquake (M_w 9.0), we determined a new detailed P-wave tomography of the Tohoku forearc, which shows a high correlation with the residual topography and gravity anomalies in the region. Our results suggest that structural heterogeneities in and around the megathrust zone control the rupture process of the Tohoku-oki earthquake. Its mainshock nucleated at a high-V, high-Q, and strong-coupling patch that probably forms a large asperity (or a cluster of asperities) in the megathrust zone. Its coseismic slip area generally exhibits normal- to high-V anomalies, which reflect granitic batholiths in the overriding plate and structural anomalies atop the subducting plate, such as fewer sediments there. Obvious high-V patches are also visible at sites of strong coseismic high-frequency radiation, whereas large afterslips occurred in low-V patches of the megathrust zone. These results indicate a clear relationship between the fault slip behavior in the Tohoku megathrust and seismic velocity variations in the upper plate and atop the lower plate.

MATERIALS AND METHODS

Seismic tomography

We applied a tomographic method (*18*, *47*) to invert 144,354 P-wave arrival-time data recorded at 382 permanent seismic stations in Tohoku from 4760 local shallow- and intermediate-depth earthquakes that occurred during January 2000 to June 2016 (Fig. 1). Lateral depth variations of the Conrad and Moho discontinuities in the overriding Okhotsk plate and the UBP were considered, and they were fixed in the tomographic inversion, because the existence of the three discontinuities in the study region has been established well and their geometries have been determined reliably (*18*, *47*). A 3D grid with a lateral-grid interval of 0.5° was set up in the modeling space to express the 3D V_p structure. The grid nodes were arranged at depths of 0 to 60 km with a vertical grid interval of 5 km and at depths of 60 to 200 km with a vertical grid interval of 20 to 50 km above the UBP, as well as at depths of 5, 25, and 75 km below the UBP. V_p perturbations at the grid nodes from a starting V_p model (*47*) and hypocentral parameters of the local earthquakes were taken as unknown parameters. In the starting 1D velocity model (*47*), V_p was 6.0 km/s in the upper crust and 6.7 km/s in the lower crust, and the Jeffreys-Bullen velocity model was adopted for the upper mantle. Following the previous tomographic studies in Tohoku (*3*, *4*, *47*), the initial V_p of the subducting Pacific slab was assigned to be 4% faster than the mantle velocity at the same depth. The V_p perturbation at any point in the modeling space was computed by linearly interpolating the V_p perturbations at the eight grid nodes surrounding that point. An efficient 3D ray tracing technique (*47*) was used to compute theoretical travel times and ray paths. The damped least-squares method with smoothing regularization (*47*) was used to solve the observation equations that relate the arrival-time data to the velocity and hypocentral parameters. The local earthquakes were relocated in the inversion process. The P-wave root-mean-square travel-time residuals before and after the tomographic inversion were 0.496 and 0.394 s, respectively, with a variance reduction of 37%.

After the 3D V_p model was obtained, we further determined a 2D V_p model for the overriding Okhotsk plate beneath the Tohoku forearc (Fig. 2D). For any point in the 2D forearc area above the UBP, we calculated travel times t_1 and t_3 for a vertical ray path with a length d from the UBP to Earth's surface using the 1D V_p model (*47*) and the obtained 3D V_p model, respectively. Then, the V_p anomaly $\frac{\delta V}{V_1}$ at that point was obtained using a simple relation $\frac{\delta V}{V_1} = \left(\frac{d}{t_3} - \frac{d}{t_1}\right) \Big/ \left(\frac{d}{t_1}\right)$, which is shown in Fig. 2D.

Resolution tests

Extensive checkerboard resolution tests (CRTs) and restoring resolution tests (RRTs) (*47*) were conducted to assess the adequacy of the ray coverage and to evaluate the tomographic resolution beneath the Tohoku forearc. To perform a CRT, we first assigned positive and negative V_p perturbations to the 3D grid nodes that were arranged in the model space, then calculated synthetic travel times for the checkerboard model with the same numbers of seismic stations, events, and ray paths as those in the real data set, and then inverted the synthetic data to see whether the input checkerboard model could be recovered. The procedure of the RRT is the same as that of the CRT, except for the input model that was derived from the obtained tomographic images. To simulate picking errors of the arrival-time data, we added random noise with an SD of 0.1 s to the synthetic travel times before the inversion. The results of these resolution tests indicate that our 3D V_p model has a resolution of ~50 km in the lateral direction and ~5 to 10 km in depth in and around the UBP (figs. S2 to S7). The 2D V_p model of the overriding Okhotsk plate also has a lateral resolution of ~50 km, because it was derived from the 3D V_p model. The test results show that fine details of the V_p structure around the megathrust can indeed be resolved independently from the V_p structure of the overriding plate.

SUPPLEMENTARY MATERIALS

Supplementary material for this article is available at http://advances.sciencemag.org/cgi/content/full/4/6/eaat4396/DC1

fig. S1. Seismograms and ray paths of sP depth phases.
fig. S2. Results of the first CRT for V_p tomography.
fig. S3. Results of the second CRT for V_p tomography.
fig. S4. Results of the third CRT for V_p tomography.
fig. S5. Results of the first RRT for V_p tomography.
fig. S6. Results of the second RRT for V_p tomography.
fig. S7. Results of the third RRT for V_p tomography.
fig. S8. Correlation coefficients between four different anomalies beneath the Tohoku forearc.
fig. S9. Along-trench variations of the subducting sediment thickness revealed by active-source seismic profiles.
fig. S10. Structural heterogeneity beneath the Tohoku forearc and characteristics of the 2011 Tohoku-oki earthquake.

REFERENCES AND NOTES

1. T. Iinuma, R. Hino, M. Kido, D. Inazu, Y. Osada, Y. Ito, M. Ohzono, H. Tsushima, S. Suzuki, H. Fujimoto, S. Miura, Coseismic slip distribution of the 2011 off the Pacific Coast of Tohoku Earthquake (M9.0) refined by means of seafloor geodetic data. *J. Geophys. Res.* **117**, B07409 (2012).
2. S. Kita, T. Okada, A. Hasegawa, J. Nakajima, T. Matsuzawa, Existence of interplane earthquakes and neutral stress boundary between the upper and lower planes of the double seismic zone beneath Tohoku and Hokkaido, northeastern Japan. *Tectonophysics* **496**, 68–82 (2010).
3. Z. Huang, D. Zhao, L. Wang, Seismic heterogeneity and anisotropy of the Honshu arc from the Japan Trench to the Japan Sea. *Geophys. J. Int.* **184**, 1428–1444 (2011).
4. D. Zhao, Z. Huang, N. Umino, A. Hasegawa, H. Kanamori, Structural heterogeneity in the megathrust zone and mechanism of the 2011 Tohoku-oki earthquake (Mw 9.0). *Geophys. Res. Lett.* **38**, L17308 (2011).
5. Y. Suwa, S. Miura, A. Hasegawa, T. Sato, K. Tachibana, Interplate coupling beneath NE Japan inferred from three-dimensional displacement field. *J. Geophys. Res.* **111**, B04402 (2006).
6. M. Sato, M. Fujita, Y. Matsumoto, T. Ishikawa, H. Saito, M. Mochizuki, A. Asada, Interplate coupling off northeastern Japan before the 2011 Tohoku-oki earthquake, inferred from seafloor geodetic data. *J. Geophys. Res.* **118**, 3860–3869 (2013).

7. Z. Huang, D. Zhao, Mechanism of the 2011 Tohoku-oki earthquake (Mw 9.0) and tsunami: Insight from seismic tomography. *J. Asian Earth Sci.* **70-71**, 160–168 (2013).
8. X. Liu, D. Zhao, S. Li, Seismic attenuation tomography of the Northeast Japan arc: Insight into the 2011 Tohoku earthquake (M_w 9.0) and subduction dynamics. *J. Geophys. Res.* **119**, 1094–1118 (2014).
9. X. Liu, D. Zhao, Depth-varying azimuthal anisotropy in the Tohoku subduction channel. *Earth Planet. Sci. Lett.* **473**, 33–43 (2017).
10. K. Wang, S. L. Bilek, Fault creep caused by subduction of rough seafloor relief. *Tectonophysics* **610**, 1–24 (2014).
11. X. Gao, K. Wang, Strength of stick-slip and creeping subduction megathrusts from heat flow observations. *Science* **345**, 1038–1041 (2014).
12. Q. Bletery, A. Thomas, A. W. Rempel, J. Hardebeck, Imaging shear strength along subduction faults. *Geophys. Res. Lett.* **44**, 11329–11339 (2017).
13. D. Bassett, D. Sandwell, Y. Fialko, A. Watts, Upper-plate controls on co-seismic slip in the 2011 magnitude 9.0 Tohoku-oki earthquake. *Nature* **531**, 92–96 (2016).
14. J. Hardebeck, J. Loveless, Creeping subduction zones are weaker than locked subduction zones. *Nat. Geosci.* **11**, 60–64 (2018).
15. N. Umino, A. Hasegawa, T. Matsuzawa, sP depth phase at small epicentral distances and estimated subducting plate boundary. *Geophys. J. Int.* **120**, 356–366 (1995).
16. G. Fujie, S. Miura, S. Kodaira, Y. Kaneda, M. Shinohara, K. Mochizuki, T. Kanazawa, Y. Murai, R. Hino, T. Sato, Along-trench structural variation and seismic coupling in the northern Japan subduction zone. *Earth Planets Space* **65**, 75–83 (2013).
17. Y. Yamamoto, K. Obana, S. Kodaira, R. Hino, M. Shinohara, Structural heterogeneities around the megathrust zone of the 2011 Tohoku earthquake from tomographic inversion of onshore and offshore seismic observations. *J. Geophys. Res.* **119**, 1165–1180 (2014).
18. D. Zhao, O. P. Mishra, R. Sanda, Influence of fluids and magma on earthquakes: Seismological evidence. *Phys. Earth Planet. Inter.* **132**, 249–267 (2002).
19. T. Lay, H. Kanamori, C. J. Ammon, K. D. Koper, A. R. Hutko, L. Ye, H. Yue, T. M. Rushing, Depth-varying rupture properties of subduction zone megathrust faults. *J. Geophys. Res.* **117**, B04311 (2012).
20. T. Tsuru, J.-O. Park, S. Miura, S. Kodaira, Y. Kido, T. Hayashi, Along-arc structural variation of the plate boundary at the Japan Trench margin: Implication of interplate coupling. *J. Geophys. Res.* **107**, 2357 (2002).
21. Y. Nakamura, S. Kodaira, S. Miura, C. Regalla, N. Takahashi, High-resolution seismic imaging in the Japan Trench axis area off Miyagi, northeastern Japan. *Geophys. Res. Lett.* **40**, 1713–1718 (2013).
22. Y. Ito, R. Hino, M. Kido, H. Fujimoto, Y. Osada, D. Inazu, Y. Ohta, T. Iinuma, M. Ohzono, S. Miura, M. Mishina, K. Suzuki, T. Tsuji, J. Ashi, Episodic slow slip events in the Japan subduction zone before the 2011 Tohoku-Oki earthquake. *Tectonophysics* **600**, 14–26 (2013).
23. N. Uchida, T. Iinuma, R. M. Nadeau, R. Bürgmann, R. Hino, Periodic slow slip triggers megathrust zone earthquakes in northeastern Japan. *Science* **351**, 488–492 (2016).
24. T. Matsuzawa, Y. Asano, K. Obara, Very low frequency earthquakes off the Pacific coast of Tohoku, Japan. *Geophys. Res. Lett.* **42**, 4318–4325 (2015).
25. F. M. Chester, C. Rowe, K. Ujiie, J. Kirkpatrick, C. Regalla, F. Remitti, J. C. Moore, V. Toy, M. Wolfson-Schwehr, S. Bose, J. Kameda, J. J. Mori, E. E. Brodsky, N. Eguchi, S. Toczko; Expedition 343 and 343T Scientists, Structure and composition of the plate-boundary slip zone for the 2011 Tohoku-oki earthquake. *Science* **342**, 1208–1211 (2013).
26. P. M. Fulton, E. E. Brodsky, Y. Kano, J. Mori, F. Chester, T. Ishikawa, R. N. Harris, W. Lin, N. Eguchi, S. Toczko; Expedition 343; Expedition 343T; KR13-087 Scientists, Low coseismic friction on the Tohoku-oki fault determined from temperature measurements. *Science* **342**, 1214–1217 (2013).
27. K. Ujiie, H. Tanaka, T. Saito, A. Tsutsumi, J. J. Mori, J. Kameda, E. E. Brodsky, F. M. Chester, N. Eguchi, S. Toczko; Expedition 343 and 343T Scientists, Low coseismic shear stress on the Tohoku-oki megathrust determined from laboratory experiments. *Science* **342**, 1211–1214 (2013).
28. N. Kato, S. Yoshida, A shallow strong patch model for the 2011 great Tohoku-oki earthquake: A numerical simulation. *Geophys. Res. Lett.* **38**, L00G04 (2011).
29. H. Noda, N. Lapusta, Stable creeping fault segments can become destructive as a result of dynamic weakening. *Nature* **493**, 518–521 (2013).
30. W. Tanikawa, T. Hirose, H. Mukoyoshi, O. Tadai, W. Lin, Fluid transport properties in sediments and their role in large slip near the surface of the plate boundary fault in the Japan Trench. *Earth Planet. Sci. Lett.* **382**, 150–160 (2013).
31. J. D. Kirkpatrick, C. D. Rowe, K. Ujiie, J. C. Moore, C. Regalla, F. Remitti, V. Toy, M. Wolfson-Schwehr, J. Kameda, S. Bose, F. M. Chester, Structure and lithology of the Japan Trench subduction plate boundary fault. *Tectonics* **34**, 53–69 (2015).
32. Y. Ito, M. Ikari, K. Ujiie, A. Kopf, Coseismic slip propagation on the Tohoku plate boundary fault facilitated by slip-dependent weakening during slow fault slip. *Geophys. Res. Lett.* **44**, 8749–8756 (2017).
33. C. Scholz, The rupture mode of the shallow large-slip surge of the Tohoku-oki earthquake. *Bull. Seism. Soc. Am.* **104**, 2627–2631 (2014).
34. T. Tsuji, K. Kawamura, T. Kanamatsu, T. Kasaya, K. Fujikura, Y. Ito, T. Tsuru, M. Kinoshita, Extension of continental crust by anelastic deformation during the 2011 Tohoku-oki earthquake: The role of extensional faulting in the generation of a great tsunami. *Earth Planet. Sci. Lett.* **364**, 44–58 (2013).
35. A. Hasegawa, K. Yoshida, Y. Asano, T. Okada, T. Iinuma, Y. Ito, Change in stress field after the 2011 great Tohoku-Oki earthquake. *Earth Planet. Sci. Lett.* **355-356**, 231–243 (2012).
36. W. Nakamura, N. Uchida, T. Matsuzawa, Spatial distribution of the faulting types of small earthquakes around the 2011 Tohoku-oki earthquake: A comprehensive search using template events. *J. Geophys. Res.* **121**, 2591–2607 (2016).
37. Y. Nakamura, S. Kodaira, B. J. Cook, T. Jeppson, T. Kasaya, Y. Yamamoto, Y. Hashimoto, M. Yamaguchi, K. Obana, G. Fujie, Seismic imaging and velocity structure around the JFAST drill site in the Japan Trench: Low Vp, high Vp/Vs in the transparent frontal prism. *Earth Planets Space* **66**, 121 (2014).
38. V. Gabuchian, A. J. Rosakis, H. S. Bhat, R. Madariaga, H. Kanamori, Experimental evidence that thrust earthquake ruptures might open faults. *Nature* **545**, 336–339 (2017).
39. S. Kurahashi, K. Irikura, Source model for generating strong ground motions during the 2011 off the Pacific coast of Tohoku Earthquake. *Earth Planets Space* **63**, 571–576 (2011).
40. K. D. Koper, A. R. Hutko, T. Lay, Along-dip variation of teleseismic short-period radiation from the 11 March 2011 Tohoku earthquake (M_w 9.0). *Geophys. Res. Lett.* **38**, L21309 (2011).
41. L. Ye, T. Lay, H. Kanamori, Ground shaking and seismic source spectra for large earthquakes around the megathrust fault offshore of northeastern Honshu, Japan. *Bull. Seism. Soc. Am.* **103**, 1221–1241 (2013).
42. T. Sun, K. Wang, T. Iinuma, R. Hino, J. He, H. Fujimoto, M. Kido, Y. Osada, S. Miura, Y. Ohta, Y. Hu, Prevalence of viscoelastic relaxation after the 2011 Tohoku-oki earthquake. *Nature* **514**, 84–87 (2014).
43. T. Iinuma, R. Hino, N. Uchida, W. Nakamura, M. Kido, Y. Osada, S. Miura, Seafloor observations indicate spatial separation of coseismic and postseismic slips in the 2011 Tohoku earthquake. *Nat. Commun.* **7**, 13506 (2016).
44. A. M. Freed, A. Hashima, T. W. Becker, D. A. Okaya, H. Sato, Y. Hatanaka, Resolving depth-dependent subduction zone viscosity and afterslip from postseismic displacements following the 2011 Tohoku-oki, Japan earthquake. *Earth Planet. Sci. Lett.* **459**, 279–290 (2017).
45. F. Tomita, M. Kido, Y. Ohta, T. Iinuma, R. Hino, Along-trench variation in seafloor displacements after the 2011 Tohoku earthquake. *Sci. Adv.* **3**, e1700113 (2017).
46. W. Wei, D. Zhao, J. Xu, F. Wei, G. Liu, *P* and *S* wave tomography and anisotropy in Northwest Pacific and East Asia: Constraints on stagnant slab and intraplate volcanism. *J. Geophys. Res.* **120**, 1642–1666 (2015).
47. D. Zhao, A. Hasegawa, S. Horiuchi, Tomographic imaging of P and S wave velocity structure beneath northeastern Japan. *J. Geophys. Res.* **97**, 19909–19928 (1992).
48. S. S. N. Gamage, N. Umino, A. Hasegawa, S. H. Kirby, Offshore double-planed shallow seismic zone in the NE Japan forearc region revealed by sP depth phases recorded by regional networks. *Geophys. J. Int.* **178**, 195–214 (2009).
49. K. Obana, G. Fujie, T. Takahashi, Y. Yamamoto, Y. Nakamura, S. Kodaira, N. Takahashi, Y. Kaneda, M. Shinohara, Normal-faulting earthquakes beneath the outer slope of the Japan Trench after the 2011 Tohoku earthquake: Implications for the stress regime in the incoming Pacific plate. *Geophys. Res. Lett.* **39**, L00G24 (2012).

Acknowledgments: We thank the Hi-net data center and the Japan Meteorological Agency Unified Earthquake Catalog for providing the high-quality arrival-time data used in this study (www.hinet.bosai.go.jp). We thank D. Bassett for sharing his residual topography and gravity data. We appreciate the helpful discussions with Z. Huang, S. Zhao, and L. Guo. We are very grateful to M. Ritzwoller (the Editor) and two anonymous referees who provided thoughtful review comments and suggestions that have improved this paper. **Funding:** This work was supported by the National Key R&D Plan of China (grant no. 2017YFC0601401), grants from the National Natural Science Foundation of China (41602207) and the National Program on Global Change and Air-Sea Interaction, State Oceanic Administration (GASI-GEOGE-01) to X.L., as well as grants from the Japan Society for the Promotion of Science (Kiban-S 23224012) and the Ministry of Education, Culture, Sports, Science and Technology (26106005) to D.Z. **Author contributions:** D.Z. conceived this study. X.L. and D.Z. analyzed the data and wrote the manuscript. **Competing interests:** The authors declare that they have no competing interests. **Data and materials availability:** All data needed to evaluate the conclusions in the paper are present in the paper and/or the Supplementary Materials. Additional data related to this paper may be requested from the authors.

Submitted 27 February 2018
Accepted 15 May 2018
Published 20 June 2018
10.1126/sciadv.aat4396

Citation: X. Liu, D. Zhao, Upper and lower plate controls on the great 2011 Tohoku-oki earthquake. *Sci. Adv.* **4**, eaat4396 (2018).